Improving Object Recognition for Mobile Robots by Leveraging Common-sense Knowledge Bases

Agnese Chiatti[1] Gianluca Bardaro[1] Enrico Daga[1] and Enrico Motta[1]

***Abstract*— To assist humans on tasks which require both navigation and perceptual abilities (e.g., monitoring an office space, serving customers in a coffee shop, collecting garbage in urban areas, and so forth), mobile robots are first expected to recognise the objects which are relevant to their tasks, disambiguating them from the surrounding noise and clutter. Compared to the case of stationary robots, this scenario increases the chances of misclassification, because objects are spotted from different viewpoints, under different conditions of lightning and occlusion. The top-performing object recognition methods available: (i) typically rely on the presence of abundant training examples and are conceived for (ii) highly-controlled, de-cluttered environments or (iii) for robots collecting fixed-pose views of the objects they have previously grasped. This calls for novel methods to recognise objects when only a few labelled observations are available (i.e., few-shot recognition) and which can also scale up to the scenario of moving robots. While few-shot object recognition from robot-collected images remains a challenge, the increasing availability of open common-sense knowledge has provided new tools to counteract the risk of misclassification. We show how combining Image Matching with external common-sense knowledge leads to a performance improvement on few-shot object recognition from robot-collected images.**

I. INTRODUCTION

Mobile robots can assist humans on tasks ranging from health and safety monitoring [1] to pre-emptive elderly care [2] and can be of particular help in smart environments especially, where they can act as moving sensors to facilitate a dynamic data exchange [3]. To *make sense* of their environment, however, these autonomous agents are expected to handle rapidly-evolving and often uncertain circumstances. The robot's ability to effectively recognise the objects it encounters is a crucial pre-requisite to most sense-making tasks involving mobile robots.

Let us consider the case of HanS, the Health and Safety autonomous inspector under development at the Knowledge Media Institute (KMi) [1]. HanS was conceived to autonomously identify potentially hazardous situations, e.g. the fire hazard caused by a pile of papers sitting next to a portable heater. To identify the threat, HanS would first need to autonomously recognise the objects *paper* and *electric heater*. Furthermore, it will need to recognise that the two objects are placed next to each other.

The top-performing object recognition methods available [4]–[6] are unsuitable for this real-world scenario, because they (i) require a very large number of annotated training examples to recognise each class and (ii) fall short when dealing with varying conditions of lightining, viewpoint and clutter. The first limitation has inspired a new research direction, which studies the object recognition problem in cases where only a few training examples are available (i.e., few-shot recognition) [7]–[10]. One way of tackling the few-shot recognition problem is learning how to match novel objects to their most similar support example [7], [10]. The work in [10] was focused on evaluating performance on a synthetic object collection, while the methods explored in [7] were evaluated in the case of a robotic pick-and-place system, equipped with a set of cameras capturing images of the grasped objects from a fixed pose. In the case of a mobile robot, the risk of misclassifying the observed objects is higher than in the two latter scenarios, because the objects can be spotted from different viewpoints and luminance conditions and cannot be grasped to de-clutter the scene. Nonetheless, the increasing availability of open common-sense knowledge bases [11]–[13] has opened up opportunities to leverage different data modalities (i.e., visual and textual) to help disambiguating objects that are hard to classify [14], [15]. Going back our running example, HanS could fail to recognise a *fire extinguisher*, for instance, when observing it from a different angle and mistake it for another object of similar shape and colour, e.g., a *red water bottle*. However, recognising that the fire extinguisher is hanging next to a *fire label*, together with knowing that *fire label* and *fire extinguisher* are semantically-related concepts, would allow HanS to correct its prediction online, i.e., without collecting any additional training examples.

This paper presents our main contributions with respect to:

- evaluating the configuration introduced in [10], which extends [7] by introducing weight imprinting [8], on the more challenging case of a mobile robot recognising objects in the wild. In this context, we also investigate whether classifying objects based on the top-K discounted majority votes can improve performance, instead of only considering the top-1 matches [10], [16];
- proposing a hybrid method that combines purely Machine Learning (ML) based object recognition, with external common-sense knowledge leveraged from WordNet [17], Visual Genome [18] and Conceptnet [11]: (i) to guide the correction of false predictions, (ii) without compromising the original performance. We quantitatively and qualitatively show how the proposed approach achieves both aims.

All the implemented code is available on our repository[1].

[1]Knowledge Media Institute, The Open University, United Kingdom name.surname@open.ac.uk

[1]https://github.com/kmi-robots/semantic-map-object-recognition/

II. RELATED WORK

In this Section we cover both ML-based and knowledge-based approaches to object recognition for mobile robots.

A. Few-shot object recognition

The object recognition methods which have ensured near-perfect [4]–[6] (or even above-human [19]) performance in highly controlled environments, require the access to very large amounts of manually-annotated data, which are expensive to produce. These approaches fall short on real-world scenes, comprising of different object categories, captured under varying luminance conditions, and in the presence of background noise and clutter. Moreover, they are not aligned with the scenario of a learner who builds its awareness of the environment incrementally, by relying on: (i) a prior world view based on known objects, and (ii) only a few observations of the current world state (i.e., few-shot learning). In fact, as also pointed out in [8], humans are able to recognise new objects from the very first exposure, drawing connections from their prior knowledge (i.e., cognitive imprinting). To address these limitations, recent works have emerged [7], [10], [20] that define the object recognition task as a metric learning problem, i.e., the problem of learning a feature space where image embeddings of similar objects lie relatively closer than dissimilar ones. In [7] representations for objects grasped by a robot (and opportunely separated from their surrounding clutter) are learned by similarity matching against reference product images.

B. Knowledge-based object recognition

The recent availability of large-scale and multi-modal common-sense knowledge bases [11], [13], [18], [21], has significantly aided the development of applications for natural language [22] (or scene) understanding, and (visual [23]) question answering [24]. Nonetheless, the use of common-sense knowledge to improve the perceptual capabilities of a system is still rather unexplored, especially in the context of robotic applications. In [25], [26], the knowledge from DBpedia [21] and WordNet [17] was used to help generating hypotheses about newly-encountered objects, extending perception-only based approaches such as RoboSherlock [27]. Differently from [25], [26], in this work we rely on ConceptNet [28] to measure semantic relatedness and also investigate the use of multi-modal knowledge bases like Visual Genome [18] to validate the object-object spatial relations. In particular, we hypothesise that this external knowledge can help correcting the weakest object predictions. This hypothesis is supported by recent studies in Computer Vision [14], [15], [29]–[31], which showed how external knowledge can aid object recognition. Akata et al. [29] have exploited the hierarchical and auxiliary information associated with textual class labels for zero-shot object classification. In [30], the co-occurrence of objects in image collections has effectively compensated purely textual-driven reasoning when validating object-object relationships. Introducing a notion of *semantic consistency* between objects, e.g., given by their joint spatial relationships and attributes [15], has also shown to improve object detection [14], [31]. The latter approaches use the transferred common-sense knowledge to modify the probability distribution of target classes and drive the model fine-tuning. We instead propose two complementary knowledge-based modules which can be integrated directly at testing time, i.e., without requiring any further fine-tuning, and are also compatible with non-probabilistic object recognition approaches (i.e., based on similarity matching, such as KNN).

III. PROPOSED APPROACH

The proposed architecture (Figure 1) includes two modules that exploit external knowledge bases. These are: (i) the object-object relationships relative to the floor level included in Visual Genome [18], (ii) the semantic relatedness [11] of objects recognised as spatially-close to one another. In addition, before adding external knowledge, we analyse the robot-collected images, to extract the spatial relationships between the objects in each scene. In a nutshell, this approach exploits spatial relationships both extracted from the scene and retrieved from external common-sense knowledge bases. The remainder of this Section illustrates each architectural component in detail.

A. Imprinted Image Matching

This module was derived from our PyTorch implementation of the K-net architecture [7]. The two-branch Network is fed with image streams drawn from two different domains: (i) the images collected by the robot within its real-world environment, and (ii) reference images representing the object models to be recognised. The Amazon product images used in [7] were in this case replaced by a task-agnostic dataset extended from [10]. To mitigate the risk of overfitting, as in [7], we relied on a ResNet50 pre-trained on ImageNet to model each CNN branch. Specifically, we fine-tuned the branch fed with robot-collected images and extracted features without re-training from the second branch devoted to synthetic images. The model was fed with a balanced 1:1 ratio of similar and dissimilar image pairs and optimised with respect to both the Triplet Loss [32] and the cross-entropy loss [7]. We implemented a mechanism to form more representative data triplets than those obtained through random sampling. Specifically, each robot-collected (anchor) image was paired not only with its L2-nearest product image (the "multi-anchor switch" strategy of [7]) but also with the L2-nearest example belonging to a different class, i.e., the hardest negative example to disambiguate.

The most significant difference between our approach and the baseline K-net is that our training routine exploits weight imprinting [8] in the last fully-connected layer. In other words, the L2 normalized embeddings output of the ResNet50 are scaled and averaged class-wise first, then L2 normalised again and applied directly as weights of the fully-connected layer. Another difference is that, at inference time, objects are classified based on a discounted majority voting KNN scheme. Let $c = 1, ..., N$ be the object classes of interest (i.e., $N = 25$ in this case) and $V = v_1, ..., v_t$ and $E = e_1, ..., e_h$

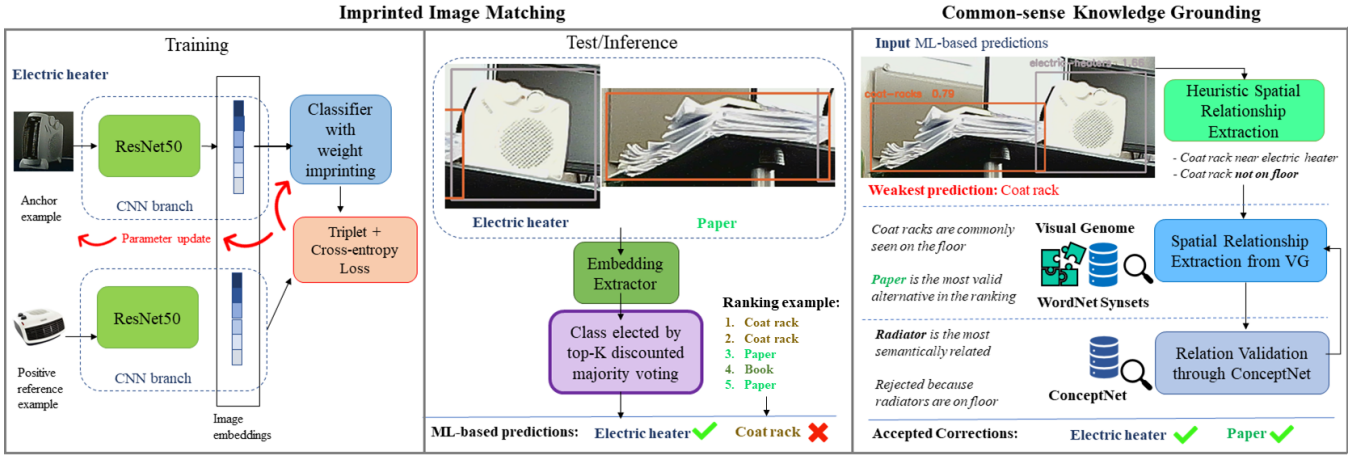

Fig. 1. The proposed approach for common-sense knowledge-grounded object recognition (Kground Imprinted K-net).

the test and train embeddings sets respectively. Results are first ranked by descending cosine similarity between the input test embedding (v_t) and embeddings in E. Then, for each c in the top-K results, a weighted score s_c is defined as:

$$s_c = \sum_{i=0}^{n_c} \frac{\cos(v_t, e_i)}{k} \tag{1}$$

where n_c is the number of times c appeared in the ranking (i.e., K is its upper bound), and k=1,...,K is the ranking position of each class label appearance. Ultimately, the predicted object class is the c for which maximum s_c applies. As all $\cos(v_t, e_i) \in [0, 1]$, the derived scores are also normalised and can be used as indicator of the algorithm's recognition confidence.

B. Heuristic Spatial Relationship Extraction from Images

Once the objects within a particular image have been recognised, the instance with minimum associated confidence score is examined. In particular, only objects with score lower than σ are considered for correction, to reduce the risk of correcting the true predictions. A first heuristic is applied to estimate whether the object is lying on the floor or not, based on the coordinates of its bounding box. Specifically, the system will conclude that an object is lying on the floor if the bottom edge of its bounding box lies within the lowest portion of the scene, defined as a fraction ρ of the image height. For example, the paper pile in Figure 1 is lying above the lowest third of the scene and will thus be marked as *paper not on floor*. This trivial yet effective heuristic was found to be quite robust in the case of a camera sensor installed on a mobile robot, i.e., kept at fixed height from the ground level. If more than one object is detected in the same scene, the system will then extract the position of the considered object with respect to the other objects found nearby. At this stage, we consider only the nearby objects the Image Matching module is reasonably confident about (i.e., with associated confidence greater or equal to σ). Let (x_{At}, y_{At}) and (x_{Ab}, y_{Ab}) be the top-left and bottom-right coordinates of region object A, so that $x_{Ab} > x_{At}$ and $y_{Ab} > y_{At}$. If (x_{Bc}, y_{Bc}) are the center-coordinates of object region B, then the spatial relation linking A to B is defined as:

$$r_{A,B} = \begin{cases} A \text{ on } B, & \text{if } x_{Bc} \in [x_{At} - \epsilon_h, x_{Ab} + \epsilon_h], \\ & y_{Bc} > y_{Ab} \\ A \text{ near } B, & \text{if } x_{Bc} \in [x_{At} - \epsilon_h, x_{Ab} + \epsilon_h], \\ & y_{Bc} \in [y_{Atop} - \epsilon_v, y_{Ab} + \epsilon_v] \\ A \text{ under } B, & \text{if } x_{Bc} \in [x_{At} - \epsilon_h, x_{Ab} + \epsilon_h], \\ & y_{Bc} < y_{At} \\ None, & \text{otherwise} \end{cases} \tag{2}$$

where ϵ_h and ϵ_v are horizontal and vertical tolerance values in pixels, and $\epsilon_v << \epsilon_h$ (objects marked as *near* lie at comparable heights). In the running example, *paper* would be found *near electric heater* (Figure 1).

C. Spatial Relationship Extraction from Visual Genome

The floor-level relationships extracted for each object at the prior stage (i.e., *object on floor/object not on floor*), are here grounded with respect to object-object relationships found in Visual Genome (VG) [18]. In particular, we consider the relationship between the object under analysis and two reference synsets: *floor.n.01* and *table.n.02*. The grounding module compares the number of times an object was found on the floor with respect to on the table, within VG, to check the validity of the detected floor-level position. In the example in Figure 1, papers were mistaken for a coat rack, however the relation *coat rack not on floor* triggers an anomaly. This is because, the relationship knowledge base indicates that a coat rack was seen on the floor but never on a table. The same trigger applies for objects appearing more often on the floor than above ground. Conversely, the presence of an object which is commonly found as often on the floor as above ground (e.g., a desktop PC) would have not triggered any anomaly. Once the anomaly is raised, the remaining K-1 predictions in the top-K ranking for coat rack are examined. At this stage, the alternative classes appearing in the ranking are scanned in descending order of confidence, in search for an object that *makes more sense* at that location.

In our example, papers are found to be the best alternative available in the ranking, as papers are commonly found on tables more often than on the floor.

D. Relation Validation through ConceptNet

The second knowledge-grounding module is activated only if no correction was applied during the prior stage. More specifically, here we intervene only on objects: (i) whose spatial relationships with respect to the ground was validated through VG, (ii) which were never observed in VG (e.g., fire labels), or (iii) whose class is an Out of Vocabulary (OOV) term with respect to WordNet (e.g., emergency exit sign). Moreover, we only analyse scenes depicting more than one object, i.e., for which a set of object-object spatial relations is available (Section III-B). This is, however, the most common type of scenes in a real-world, cluttered environment. For all images meeting the above criteria, the top-K ranking related to the weakest object prediction is examined. Each class appearing in the ranking is compared against the other M objects found nearby, to compute their pairwise semantic relatedness. This is given by the similarity of the two word embeddings under comparison [11] and other relations in the ConceptNet graph [28]. Conveniently, this API can estimate word embeddings even for OOV words, by averaging the vectors of neighbour terms in the ConceptNet graph, making this module highly scalable to many object classes and applications. Formally, we compute the cumulative semantic relatedness of class c in the ranking with respect to all objects found *on*, *under* or *nearby* as follows:

$$s_{sem,c} = \sum_{i=0}^{n_c} \sum_{j=1}^{M} sem_{rel}(syn_c, syn_{m_j}) \tag{3}$$

where n_c is the number of times c appeared in the ranking, and $sem_{rel}(c, m_j)$ is the semantic relatedness score between class c and a nearby object m_j. Ultimately, the c for which maximum $s_{sem,c}$ applies is proposed for correction.

The new label proposed for correction will need to be validated, based on its position with respect to the floor. Thus, a similar check to the one illustrated in Section III-C is performed, this time to assess if the difference between the counts associated to the original label and the proposed correction differ by more than δ. This simple heuristic is used to estimate whether the original object and the new candidate have a similar spatial relationship with respect to the floor (i.e., both are found on the floor, or both can indifferently be found on the floor or on a table). Hence, the correction will be applied only if the proposed class passes this validation check. For instance, *radiator* would not be an acceptable label for a pile of paper spotted on a desk.

IV. EXPERIMENTS

A. Data Preparation

KMiSet. We collected images in the Knowledge Media Institute (KMi) office environment through a Turtlebot mounting an Orbbec Astra Pro RGB-D monocular camera. Images were labelled with respected to a taxonomy of 25 object classes (Figure 3), five of which are specific to the Health and Safety use-case of interest [1]: i.e., fire extinguisher, fire (extinguisher) label, electric heater, power cord and emergency exit sign. First, we collected five pictures of each target object individually, in a de-cluttered Lab environment. Each image was manually-cropped to reduce the marginal noise. In the following, we refer to this set as *KMiSet-ref*. We used a 4/1 training/validation split on KMiSet-ref to fine-tune the Imprinted Image Matching Network.

For testing purposes, additional 295 RGB images (accounting for 896 object instance, or bounding boxes) were collected by the robot while navigating in KMi, this time without constraining the number of objects captured per frame and without removing clutter. Images were stored at their maximum resolution (i.e., 1280x720) and annotated through the VGG Image Annotation (VIA) open-source tool [33], to keep track of both the rectangular regions enclosing each object and their associated class. In the following, we refer to this set as *KMiSet-test*. Class cardinalities in KMiSet-test resemble the relative occurrence of objects in the considered domain (e.g., HanS is likely to encounter fire extinguishers and people more often than windows, on its scouting round) and were thus kept as-is, i.e., without re-sampling, as noticeable from the class supports in Figure 3).

ShapeNet+Google-25class (SNG-25). Here we extended the SNG-20 dataset introduced in [10] to include 25 classes, following the same data preparation protocol as in [10].

Visual Genome relationships. Visual Genome [18] is a large collection of 108'077 natural images from the intersection of YFCC100M [34] and MS-COCO [35]. Here each provided region is annotated with respect to: (i) the object class label, (iii) the canonicalised WordNet synset related to that label, (iv) a textual description of the region content, and, optionally, (v) additional object attributes (e.g., colour, state, and others). Moreover, for each image: (vi) the object-object relationships connecting different object regions, and (vii) a set of sample Q&A about the scene, are also provided. Since we focused on spatial relationships (e.g., *cup on floor* as opposed to *man wear hat*), we parsed the imageID-centric representation offered in the latest VG release (v.1.4) to a more spatially-centric format. First, we indexed all relationships (spatial and non-spatial) in VG through their predicate (e.g., *on*, *has*, *wears*, etc.). Second, each predicate was linked to all its known aliases (e.g., *next to* and *around* were merged under their common reference *near*). Then, within each predicate, relationships were grouped based on their unique subject-object pair and linked to their occurrence count (e.g., for the *'on'* predicate, the *'book.n.01-shelf.n.01'* pair recurred 1228 times). Specifically, we represented subjects and objects through their canonicalised synsets [18], to normalise alternative annotations describing the same concept. In this way, e.g., instances labelled *book*, *account book* and *volume* are all reconciled under the *book.n.01* synset. Concurrently, we discarded compound sentences (e.g., **subject:** *green trees seen* - **predicate:** *green trees by road*, **object:** *trees on roadside*), which are out of the scope of this work.

B. Ablation study

This Section describes the different configurations under comparison and the architectural components modified before each performance assessment. The evaluation was conducted on manually-annotated bounding boxes, to control for errors typically propagated from the object detection process. However, this framework can be similarly applied to any workflow that provides rectangular object regions.

Baseline NN is the chosen baseline, where features describing the KMiSet images are extracted from a ResNet50 pre-trained on ImageNet without re-training. In particular, the embeddings extracted for KMiSet-test are matched to their L2 Nearest Neighbour in KMiSet-ref.

K-net is our implementation of the two-branch network optimised for known object classes in [7]. Here we fed the product image branch with 2D views in the SNG-25 dataset.

Imprinted K-net is the component in Section III-A.

Imprinted K-net + ConceptRel also integrates the ConceptNet-based component described in Section III-D.

Kground Imprinted K-net is the architecture proposed in Section III. It extends Imprinted K-net + ConceptRel with two additional validation steps based on Visual Genome.

C. Implementation Details

The input images were resized to 224x224 and normalised to the same distribution as the ImageNet-1000 dataset (used for pre-training each ResNet50 module). For all tested configurations, the robot-collected image branch was fine-tuned with minibatch Gradient Descend on 16 image pairs per batch, with learning rate set to 0.0001, momentum 0.9 and weight decay 0.00001. Parameters were updated for up to 5000 epochs, with an early stopping whenever the validation loss had not decreased for more than 100 iterations. For both the knowledge-based modules, we tested out different threshold values and found the best configuration to be: $\sigma =$ 1.14 (i.e., 50% confidence), $\rho = 1/3$, $\epsilon_v =$10 pixels and $\delta =$ 80. Moreover, we set ϵ_h to be dynamically equal to the width of each bounding box eligible for correction.

V. RESULTS AND DISCUSSION

A. Quantitative Evaluation

The cumulative results obtained on KMiSet-test are reported in Table I. Since KMiSet-test is worth a different number of object examples for each class, here the cross-class cumulative performance is defined in terms of average Precision Recall and F-1 score, with averages weighted by class support. All configurations that involved fine-tuning on the KMiSet-ref set, consisting of only 5 reference shots per class, ensured a higher performance than the baseline NN approach. Moreover, introducing weight imprinting [8] in the K-net architecture [7] led to an increment in the overall accuracy and F1-score. An additional improvement was achieved by introducing a discounted majority voting scheme in the inference process (following Equation 1). Based on these results, we considered the Imprinted K-net with discounted majority voting as baseline for our further performance assessments.

TABLE I
CROSS-CLASS RESULTS ON KMISET-TEST

Approach	Accuracy	Precision	Recall	F1
Top-1				
Baseline NN	0.63	0.76	0.63	0.63
K-net [7]	0.63	**0.80**	0.63	0.65
Imprinted K-net	0.65	0.76	0.65	0.66
Top-5 (majority voting)				
Imprinted K-net	0.64	0.76	0.64	0.66
Top-5 (discounted majority voting)				
Imprinted K-net	0.65	0.77	0.65	0.66
Imprinted K-net + ConceptRel	**0.66**	0.77	**0.66**	0.67
Kground Imprinted K-net	**0.66**	0.78	**0.66**	**0.68**

Indeed, introducing the ConceptNet-based correction routine alone introduced a slight performance improvement. However, the addition of two floor-level grounding modules based on Visual Genome further benefited the results, exceeding the baseline F-1 score by 2%. Moreover, the class-wise results (Figure 3) suggest that, in the latter configuration, corrections were applied more conservatively than when relying exclusively on ConceptNet. In fact, for most classes, the obtained F-1 was higher than in the absence of external common-sense knowledge, or comparable to it. Overall, the proposed approach could complement the purely ML-based methods, without undermining their baseline performance.

B. Qualitative Evaluation and Error Analysis

Figure 2 provides a sample comparison between the original predictions returned by the Imprinted K-net with discounted majority voting and the predictions obtained after integrating each knowledge-based module. The qualitative results obtained were grouped along three rows, to assess: (i) whether the common-sense knowledge grounding module (a) managed (b) or did not manage to correct those predictions that actually needed correction (false predictions); (ii) while also preserving the predictions that did not need correction (true predictions). Below each scene, the weakest prediction is indicated for comparison. By definition, corrections were viable only in scenarios where a correct alternative to the original prediction actually appeared in the top-5 ranking. Therefore, both knowledge-based methods were not able to counteract all cases where a specific object had been prior misclassified with high confidence, or up to its top-K ranking. This is the case of the *paper bin* mistaken for a *mug*, in row (i.b). Similarly, our system failed to correct all false predictions that could not be disambiguated by just looking at spatial relations. For instance, if a monitor was mistaken for a desktop computer, the prediction would be accepted, because computers can be found as often above as below desks. Interestingly, in other cases, introducing a knowledge-grounding mechanism helped guiding the correction towards classes which were more semantically related to the ground truth class. For example, the *electric heater* in row (i.b) was first mistaken for a *bin*, but later corrected as a *desktop computer*. Even though *computer* is certainly not the true prediction, *bin* was still modified in favour of a class of objects which is commonly equipped with a *power cord*, after recognising that *object is located near a power cord*.

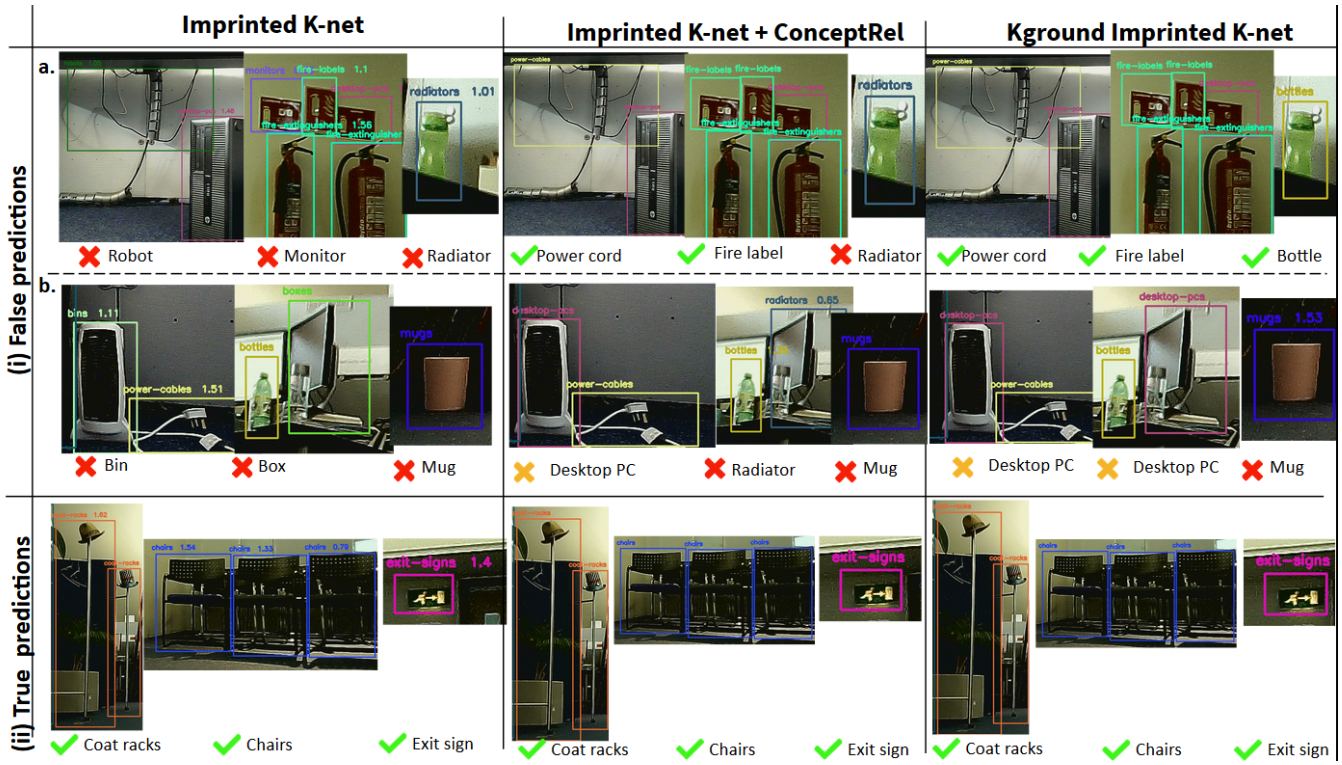

Fig. 2. Examples of corrections applied to the Imprinted K-net predictions after integrating each knowledge-based module.

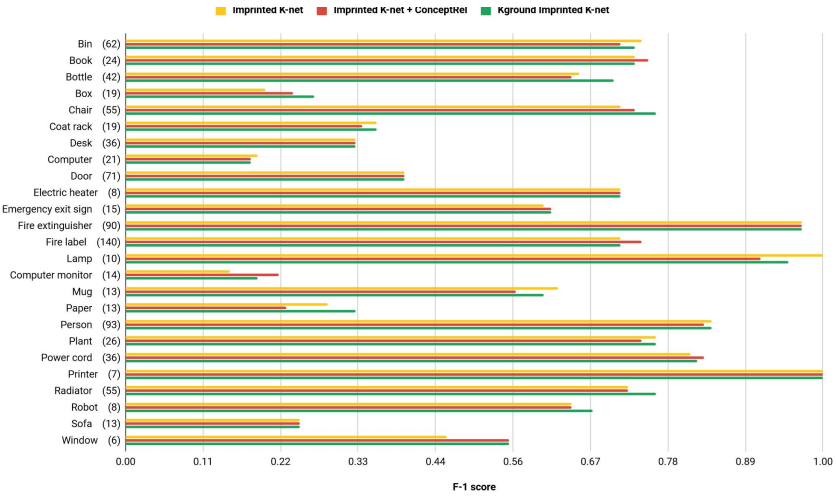

Fig. 3. Class-wise F-1 scores on KMiSet-test. Each label is accompanied by the class support.

VI. CONCLUSION AND FUTURE WORK

We presented an object recognition approach that extends [10] by integrating common-sense knowledge from ConceptNet [36], WordNet [17] and Visual Genome [18]. We evaluated the proposed approach on a test set collected by a mobile robot in a real-world office environment and compared against the state-of-the-art methods introduced for known object classes in [7]. The proposed architecture led to a 2% overall improvement on the F1 score, without compromising the baseline performance (i.e., achieved in the absence of common-sense knowledge). Nonetheless, the error analysis described in Section V-B highlighted the limitations affecting our current approach, which will inform our future work. First, the heuristics applied to extract the target spatial relationships in a given scene could be further refined, for instance by capitalising on the depth data collected by the robot to more accurately detect the object relative positions. Moreover, we intend to explore how: (i) the robot's initial object representations collected here can be reused to inform future predictions, i.e., in an incremental fashion [25], [26], (ii) additional object properties (e.g., attributes in VG) and open knowledge bases can be effectively integrated within the current architecture.

REFERENCES

[1] E. Bastianelli, G. Bardaro, I. Tiddi, and E. Motta, "Meet hans, the health&safety autonomous inspector," in *Proceedings of the ISWC 2018 Posters & Demonstrations, Industry and Blue Sky Ideas Tracks, 17th International Semantic Web Conference (ISWC 2018), Monterey (CA), United States.* CEUR Workshop Proceedings, 2018.

[2] M. Bajones, D. Fischinger, A. Weiss, D. Wolf, M. Vincze, P. de la Puente, T. Körtner, M. Weninger, K. Papoutsakis, D. Michel, *et al.*, "Hobbit: Providing fall detection and prevention for the elderly in the real world," *Journal of Robotics*, vol. 2018, 2018.

[3] I. Tiddi, E. Bastianelli, E. Daga, M. dAquin, and E. Motta, "Robot–city interaction: Mapping the research landscapea survey of the interactions between robots and modern cities," *International Journal of Social Robotics*, pp. 1–26, 2019.

[4] J. Redmon, S. Divvala, R. Girshick, and A. Farhadi, "You only look once: Unified, real-time object detection," in *Proceedings of the IEEE conference on computer vision and pattern recognition*, 2016, pp. 779–788.

[5] S. Ren, K. He, R. Girshick, and J. Sun, "Faster r-cnn: towards real-time object detection with region proposal networks," *IEEE Transactions on Pattern Analysis & Machine Intelligence*, no. 6, pp. 1137–1149, 2017.

[6] W. Liu, D. Anguelov, D. Erhan, C. Szegedy, S. Reed, C.-Y. Fu, and A. C. Berg, "Ssd: Single shot multibox detector," in *European conference on computer vision*. Springer, 2016, pp. 21–37.

[7] A. Zeng, S. Song, K.-T. Yu, E. Donlon, F. R. Hogan, M. Bauza, D. Ma, O. Taylor, M. Liu, E. Romo, *et al.*, "Robotic pick-and-place of novel objects in clutter with multi-affordance grasping and cross-domain image matching," in *2018 IEEE International Conference on Robotics and Automation (ICRA)*. IEEE, 2018, pp. 1–8.

[8] H. Qi, M. Brown, and D. G. Lowe, "Low-shot learning with imprinted weights," in *Proceedings of the IEEE Conference on Computer Vision and Pattern Recognition*, 2018, pp. 5822–5830.

[9] F. Sung, Y. Yang, L. Zhang, T. Xiang, P. H. Torr, and T. M. Hospedales, "Learning to compare: Relation network for few-shot learning," in *Proceedings of the IEEE Conference on Computer Vision and Pattern Recognition*, 2018, pp. 1199–1208.

[10] A. Chiatti, G. Bardaro, E. Bastianelli, I. Tiddi, P. Mitra, and E. Motta, "Task-agnostic object recognition for mobile robots through few-shot image matching," *Pre-print available at https://robots.kmi.open.ac.uk/preprints/Special_Issue___Extension_of_DARLI_AP_2019.pdf*, 2019.

[11] R. Speer and J. Lowry-Duda, "Conceptnet at semeval-2017 task 2: Extending word embeddings with multilingual relational knowledge," in *Proceedings of the 11th International Workshop on Semantic Evaluation (SemEval-2017), at ACL 2017*. ACM, 2017, pp. 85–89.

[12] M.-K. Hu, "Visual pattern recognition by moment invariants," *IRE transactions on information theory*, vol. 8, no. 2, pp. 179–187, 1962.

[13] M. K. Bergman, "Modular, expandable typologies," in *A Knowledge Representation Practionary*. Springer, 2018, pp. 207–226.

[14] Y. Fang, K. Kuan, J. Lin, C. Tan, and V. Chandrasekhar, "Object detection meets knowledge graphs," in *Proceedings of the Twenty-Sixth International Joint Conference on Artificial Intelligence, IJCAI-17*, 2017, pp. 1661–1667.

[15] K. Kumar Singh, S. Divvala, A. Farhadi, and Y. Jae Lee, "Dock: Detecting objects by transferring common-sense knowledge," in *Proceedings of the European Conference on Computer Vision (ECCV)*, 2018, pp. 492–508.

[16] K. Zheng, A. Pronobis, and R. P. Rao, "Learning graph-structured sum-product networks for probabilistic semantic maps," in *Proceedings of the 32nd AAAI Conference on Artificial Intelligence (AAAI), New Orleans, LA, USA.(Cited on pages 21 and 22.)*, 2018.

[17] G. A. Miller, "Wordnet: a lexical database for english," *Communications of the ACM*, vol. 38, no. 11, pp. 39–41, 1995.

[18] R. Krishna, Y. Zhu, O. Groth, J. Johnson, K. Hata, J. Kravitz, S. Chen, Y. Kalantidis, L.-J. Li, D. A. Shamma, *et al.*, "Visual genome: Connecting language and vision using crowdsourced dense image annotations," *International Journal of Computer Vision*, vol. 123, no. 1, pp. 32–73, 2017.

[19] O. Russakovsky, J. Deng, H. Su, J. Krause, S. Satheesh, S. Ma, Z. Huang, A. Karpathy, A. Khosla, M. Bernstein, *et al.*, "Imagenet large scale visual recognition challenge," *International Journal of Computer Vision*, vol. 115, no. 3, pp. 211–252, 2015.

[20] G. Koch, R. Zemel, and R. Salakhutdinov, "Siamese neural networks for one-shot image recognition," in *ICML deep learning workshop*, vol. 2, 2015.

[21] S. Auer, C. Bizer, G. Kobilarov, J. Lehmann, R. Cyganiak, and Z. Ives, "Dbpedia: A nucleus for a web of open data," in *The semantic web*. Springer, 2007, pp. 722–735.

[22] S. Storks, Q. Gao, and J. Y. Chai, "Commonsense reasoning for natural language understanding: A survey of benchmarks, resources, and approaches," *arXiv preprint arXiv:1904.01172*, 2019.

[23] R. Zellers, Y. Bisk, A. Farhadi, and Y. Choi, "From recognition to cognition: Visual commonsense reasoning," in *The IEEE Conference on Computer Vision and Pattern Recognition (CVPR)*, June 2019.

[24] V. Lopez, M. Fernández, E. Motta, and N. Stieler, "Poweraqua: Supporting users in querying and exploring the semantic web," *Semantic Web*, vol. 3, no. 3, pp. 249–265, 2012.

[25] J. Young, V. Basile, L. Kunze, E. Cabrio, and N. Hawes, "Towards lifelong object learning by integrating situated robot perception and semantic web mining," in *Proceedings of the Twenty-second European Conference on Artificial Intelligence*. IOS Press, 2016, pp. 1458–1466.

[26] J. Young, L. Kunze, V. Basile, E. Cabrio, N. Hawes, and B. Caputo, "Semantic web-mining and deep vision for lifelong object discovery," in *2017 IEEE International Conference on Robotics and Automation (ICRA)*. IEEE, 2017, pp. 2774–2779.

[27] M. Beetz, F. Bálint-Benczédi, N. Blodow, D. Nyga, T. Wiedemeyer, and Z.-C. Marton, "Robosherlock: Unstructured information processing for robot perception," in *2015 IEEE International Conference on Robotics and Automation (ICRA)*. IEEE, 2015, pp. 1549–1556.

[28] R. Speer, J. Chin, and C. Havasi, "Conceptnet 5.5: An open multilingual graph of general knowledge." in *AAAI*, 2017, pp. 4444–4451.

[29] Z. Akata, F. Perronnin, Z. Harchaoui, and C. Schmid, "Label-embedding for image classification," *IEEE transactions on pattern analysis and machine intelligence*, vol. 38, no. 7, pp. 1425–1438, 2015.

[30] F. Sadeghi, S. K. Kumar Divvala, and A. Farhadi, "Viske: Visual knowledge extraction and question answering by visual verification of relation phrases," in *Proceedings of the IEEE conference on computer vision and pattern recognition*, 2015, pp. 1456–1464.

[31] F. Yuan, Z. Wang, J. Lin, L. F. D'Haro, K. J. Jae, Z. Zeng, and V. Chandrasekhar, "End-to-end video classification with knowledge graphs," *arXiv preprint arXiv:1711.01714*, 2017.

[32] F. Schroff, D. Kalenichenko, and J. Philbin, "Facenet: A unified embedding for face recognition and clustering," in *Proceedings of the IEEE conference on computer vision and pattern recognition*, 2015, pp. 815–823.

[33] A. Dutta and A. Zisserman, "The VIA annotation software for images, audio and video," *arXiv preprint arXiv:1904.10699*, 2019.

[34] B. Thomee, D. A. Shamma, G. Friedland, B. Elizalde, K. Ni, D. Poland, D. Borth, and L.-J. Li, "Yfcc100m: The new data in multimedia research," *Commun. ACM*, vol. 59, no. 2, pp. 64–73, Jan. 2016.

[35] T.-Y. Lin, M. Maire, S. Belongie, J. Hays, P. Perona, D. Ramanan, P. Dollár, and C. L. Zitnick, "Microsoft coco: Common objects in context," in *European conference on computer vision*. Springer, 2014, pp. 740–755.

[36] E. Nunes and M. L. Gini, "Multi-robot auctions for allocation of tasks with temporal constraints." in *AAAI*, 2015, pp. 2110–2116.